# Electromagnetic Inverse Problem for Relaxation Time Distribution in the Time-Domain

Megan J. Armentrout*
Oregon State University

Advisor: Professor Nathan L. Gibson

June 16, 2011

**Abstract**

We consider wide bandwidth electromagnetic pulse interrogation problems for the determination of dielectric response parameters in complex dispersive materials. We couple Maxwell's equations with an auxiliary ODE modeling dielectric polarization. A problem of particular interest is to identify parameters in a standard polarization model (e.g., Debye or Lorentz) using time-domain electric field data. A larger class of materials (e.g., anomalously dispersive media) can be represented by assuming distributions of parameters (e.g., relaxation times). We present results from an inverse problem for the relaxation time distribution based on a least squares cost functional and utilizing generalized Polynomial Chaos in the forward problem.

## 1 Introduction

Electromagnetic (EM) waves are a part of everyday life. There are many applications in which EM waves pass through dielectric materials, for example, in cancer detection, cellphone usage and terahertz radiation used in airport security screening. In these and other applications, an electromagnetic wave is sent through a dielectric (non-conductive) material- sometimes a human being. People have been trying to understand what happens to EM waves when they are introduced into materials for at least the last century [8]. Not only do scientists want to know what is happening, but a great advantage comes from being able to mathematically model the situation. In some applications, it is of interest to be able to know the properties of a material by looking at how the electric or magnetic field has been altered after it has passed through it. For example, in cancer detection, the use of ultrawideband(UWB) microwave pulses can sometimes be used to determine what is inside someone's body without resorting to surgery. So, it is of use to have methods that determine properties of a substance without needing to perform extensive experiments on it.

This paper focuses on using Maxwell's equations in a dispersive dielectric media, for example a Debye media. A material is dispersive if its permittivity and/or conductivity is dependent on the angular frequency of the waves passing through it. When an electric field is induced on a dielectric, the molecules become polarized and align accordingly. When the field is removed, the molecules return to their equilibrium position. The average time it takes for the molecules in the dielectric to return to equilibrium once the electric field is removed is called the relaxation time. This is a parameter of the material. The Debye model, which was published in 1929 [8] assumes the relaxation time is a scalar. This method is very popular and fits the data well for some materials. We refer to materials for which the Debye model is not a good fit as anomalously dispersive. Von Schweidler [10], in 1907 observed that multiple relaxation times are exhibited in experimental data. And in 1913, Wagner [11] suggested modeling with a continuous distribution of relaxation times. For instance, Cole-Cole method [7] provides a better fit to true data than Debye, and uses a continuous distribution of relaxation times. The Cole-Cole model corresponds to fractional order

*armentrm@math.oregonstate.edu

differential equations, and therefore is difficult to simulate. In [4], a uniform distribution of the relaxation time is used to fit to the true data. They show that the uniformly distributed permittivity fits the true data better than the Debye model, but not as well as the Cole-Cole model. It has also been observed that the distribution of relaxation times resembles a log-normal distribution [6]. Since the beta distribution can resemble a log-normal distribution, and has some nicer properties and finite support, in this paper we will assume the relaxation times follow a beta distribution.

Broadband wave propagation is most conveniently simulated in the time domain. Therefore, in Section 2 we describe Maxwell's equations for the forward propagation of an interrogating source in an anomalously dispersive media described in terms of a *random polarization*. A numerical discretization method is defined in Section 4. An inverse problem for the distributions representing material parameters is introduced in Section 5. Finally, numerical results for specific cases of the inverse problem are presented and discussed in Section 6.

# 2 Background

## 2.1 Maxwell's Equations

Maxwell's equations govern the behavior of EM fields. These are fundamental equations when studying how the electric field, $\mathbf{E}$, and the magnetic field, $\mathbf{H}$ behave and affect the materials they pass through. These equations are given in their differential form as

$$\frac{\partial \mathbf{D}}{\partial t} + \mathbf{J} = \nabla \times \mathbf{H} \tag{1}$$

$$\frac{\partial \mathbf{B}}{\partial t} = -\nabla \times \mathbf{E} \tag{2}$$

$$\nabla \cdot \mathbf{D} = \rho \tag{3}$$

$$\nabla \cdot \mathbf{B} = 0. \tag{4}$$

In the above equations, the electric and magnetic flux densities are represented by $\mathbf{D}$ and $\mathbf{B}$, respectively. The scalar, $\rho$ is the density of free electric charges that are unaccounted for in the electric polarization. The conduction current density is given by $\mathbf{J}$. Maxwell's Equations are completed by the constitutive laws. These laws describe the response of the medium to the electromagnetic field and are given by

$$\mathbf{D} = \varepsilon \mathbf{E} + \mathbf{P} \tag{5}$$

$$\mathbf{B} = \mu \mathbf{H} + \mathbf{M} \tag{6}$$

$$\mathbf{J} = \sigma \mathbf{E} + \mathbf{J}_s. \tag{7}$$

In the above equations, the macroscopic polarization is given by $\mathbf{P}$, the magnetization, $\mathbf{M}$, and the source current density is $\mathbf{J_s}$. The electric permittivity, $\varepsilon$, is given by $\varepsilon_0 \varepsilon_r$, where $\varepsilon_0$ is the permittivity of free space and $\varepsilon_r$ is the relative permittivity of the medium. The magnetic permeability is given by $\mu$ and $\sigma$ is the electric conductivity. By combining equations (1), (5) and (7) and neglecting the source current, $\mathbf{J}_s$, we get

$$\varepsilon \frac{\partial \mathbf{E}}{\partial t} = -\sigma \mathbf{E} - \frac{\partial \mathbf{P}}{\partial t} + \nabla \times \mathbf{H}. \tag{8}$$

Assuming there is no magnetization, we combine equations (2) and (6) to get

$$\mu \frac{\partial \mathbf{H}}{\partial t} = -\nabla \times \mathbf{E}. \tag{9}$$

The behavior of EM waves can be described by their evolution in space and time. This information is needed for a simulation. The curl equations uniquely determine this behavior with the appropriate boundary and initial conditions. The methods described throughout this paper apply directly to three dimensions, however, for the purposes of simulations we will restrict the problem to one dimension. Assuming the waves propagate

in the $x$ direction, have an electric field oscillating in the $y$ direction, a magnetic field oscillating in the $z$ direction, and neglecting magnetization, equations (8) and (9) become

$$\varepsilon \frac{\partial E}{\partial t} = -\frac{\partial H}{\partial x} - \sigma E - \frac{\partial P}{\partial t} \tag{10}$$

$$\frac{\partial H}{\partial t} = -\frac{1}{\mu}\frac{\partial E}{\partial x} \tag{11}$$

where $E := \mathbf{E}_y$, $H := \mathbf{H}_z$, $P := \mathbf{P}_y$.

## 2.2 Polarization

In general, dielectrics do not polarize instantaneously. The dielectric is polarized in a way that reflects what the electric field was previously. Because of this physical fact, the polarization can be written in the convolution form,

$$\mathbf{P}(t,\mathbf{x}) = g * \mathbf{E}(t,\mathbf{x}) = \int_0^t g(t-s,\mathbf{x})\mathbf{E}(s,\mathbf{x})\mathtt{ds}, \tag{12}$$

where $g(t,\mathbf{x})$ is a dielectric response function (DRF). Dielectric response functions characterize the dielectric material by physical parameters including permittivity, $\varepsilon_\infty$,$\varepsilon_0$, and relaxation time, $\tau$. We can represent this parameter dependence by writing $g(t,\mathbf{x};\nu)$ where typically $\nu = \{\varepsilon_\infty, \varepsilon_0, \tau\}$. For Debye materials, the DRF is given by

$$g(t,\mathbf{x},\nu) = \frac{\varepsilon_0\varepsilon_d}{\tau}e^{-t/\tau} \tag{13}$$

where $\varepsilon_d = \varepsilon_s - \varepsilon_\infty$ and $\tau$ is the relaxation time. Substituting equation (12) into (5) and taking the Laplace transform in time we get,

$$\hat{\mathbf{D}} = \varepsilon(\omega)\hat{\mathbf{E}} \tag{14}$$

where $\omega$ is the angular frequency and $\varepsilon(\omega)$ is the complex permittivity. The complex permittivity is given by

$$\varepsilon(\omega) = \varepsilon_0\varepsilon_\infty + \frac{\varepsilon_0\varepsilon_d}{1+i\omega\tau}. \tag{15}$$

Using the formulation (12) with (13) can be shown to be equivalent to the solution of,

$$\tau\dot{\mathbf{P}} + \mathbf{P} = \varepsilon_0\varepsilon_d\mathbf{E} \tag{16}$$

The Debye ODE model is efficient to simulate, however it does not represent data well. Experiments and previous research have shown that better fits to data are found when the relaxation time, $\tau$, is a random variable with probability distribution (PDF). The Cole-Cole model,[7], is a generalization of the Debye model that allows $\tau$ to take the form of a distribution. The DRF for the Cole-Cole model is

$$g(t,\mathbf{x},\nu) = \frac{1}{2\pi i}\int_{\xi-i\infty}^{\xi+i\infty} \frac{\varepsilon_0\varepsilon_d}{1+(st)^{1-\alpha}}e^{st}ds. \tag{17}$$

The real part of the permittivity is shown in Figure 1 for the Debye and Cole-Cole models. Note in this figure there are multiple poles, or dips. This corresponds to multiple relaxation times within the material being tested. In [9], Gabriel performs experiments on many different biological tissues. From these experiments, the permittivity and conductivity can be plotted against the Debye and Cole-Cole models. The conductivity is shown in Figure 2 for the Debye and Cole-Cole models. As can be seen in Figures 1 and 2 plots, the Cole-Cole model better represents the data. However, problems arise in implementation. When simulating the Cole-Cole model, fractional derivatives are required to be computed, which are computationally expensive. The Cole-Cole model is equivalent to a particular distribution of relaxation times (which can be shown by the Mellon Transform). For this paper, we consider the Debye model, but with a continuous distribution of relaxation times with PDF $F(\tau)$. To allow for a distribution of relaxation times, $F$ in some admissible set, $\mathcal{N}$ generalize (12) to

$$\mathbf{P}(t,\mathbf{x}) = g * \mathbf{E}(t,\mathbf{x}) = \int_0^t \int_{\mathcal{N}} g(t-s,\mathbf{x};\nu)\mathbf{E}(s,\mathbf{x})dF(\nu)ds. \tag{18}$$

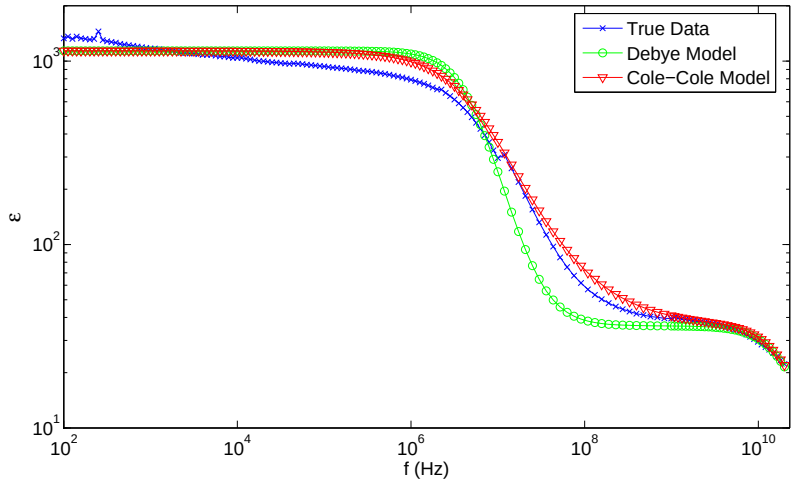


Figure 1: Permittivity for Debye and Cole-Cole Models

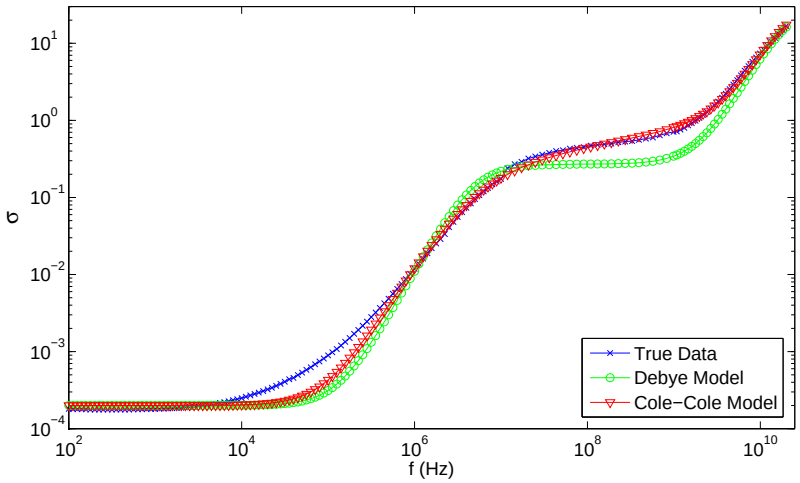


Figure 2: Conductivity for Debye and Cole-Cole Models

We choose $F$ from $\mathfrak{P}(\mathcal{N})$, the set of all probability measures on $\mathcal{N}$. It was shown in [1, 3] that (18) in Maxwell's equations is well-posed.

## 2.3 Random Polarization

The polarization in convolution form (18) is difficult to simulate, so we seek an ODE representation. Let us consider the Debye model with $\tau$ represented by a random variable with PDF $F(\tau)$.

**Definition 1.** *We define the* ***random polarization*** *to be $\mathcal{P}(t, \boldsymbol{x}; \tau)$, which can be shown to be the solution to*

$$\tau \dot{\mathcal{P}} + \mathcal{P} = \varepsilon_0 \varepsilon_d \boldsymbol{E}. \tag{19}$$

We take $\mathbf{P}(t, \mathbf{x}, F)$ to be the expected value of $\mathcal{P}(t, \mathbf{x}, \tau)$, denoted by $\mathbb{E}[\mathcal{P}(t, \mathbf{x}, \tau)]$,

$$\mathbf{P}(t, \mathbf{x}, F) = \mathbb{E}[\mathcal{P}(t, \mathbf{x}, \tau)] = \int_0^\infty \mathcal{P}(t, \mathbf{x}; \tau) dF(\tau) \tag{20}$$

$$= \int_{\tau_a}^{\tau_b} \mathcal{P}(t, \mathbf{x}; \tau) dF(\tau). \tag{21}$$

Since it is unreasonable to consider infinite or zero relaxation times, we assume relaxation times fall in an interval between some $\tau_a$ and $\tau_b$. In order to perform inverse problems involving distributions of relaxation times, efficient and accurate ways of simulating $\mathcal{P}$ and approximating $\mathbb{E}[\mathcal{P}]$ are needed. These are discussed in Sections 4.2 and 4.3.

# 3 Beta Distribution

Experimental data shows that relaxation times of a dielectric media appear to follow a log-normal distribution [6]. We assume a beta distribution, for three reasons. A beta distribution can closely resemble a log-normal distribution, beta has finite support, where log-normal does not. Also, beta allows us to use an efficient method in the forward simulation, generalized polynomial chaos. In Figure 3, it can be seen that the beta distribution can closely resemble the log-normal distribution. From a closer look, it can also be seen that the

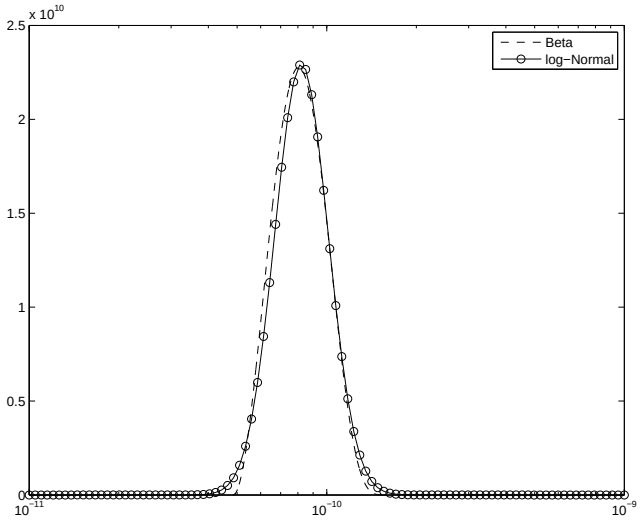


Figure 3: Beta Distribution vs. Log-Normal Distribution

beta distribution has finite support, while the log-normal distribution does not. Since we assume $\tau \in [\tau_a, \tau_b]$, modeling $\tau$ with a finitely supported distribution is more realistic (and easier computationally).

## 3.1 Standard [0,1]

The standard beta distribution has two parameters, typically referred to as $\alpha$ and $\beta$ with support [0,1]. Our notation uses $a$ and $b$ where $\alpha = b + 1$ and $\beta = a + 1$. With support [0,1], we have the following formulas for the mean, standard deviation, and PDF in terms of the beta function, $B$.

$$\mu_{s0} = \frac{\alpha}{\alpha + \beta} = \frac{b + 1}{a + b + 2} \tag{22}$$

$$\sigma_{s0}^2 = \frac{\alpha\beta}{(\alpha+\beta)^2(\alpha+\beta+1)} = \frac{(b+1)(a+1)}{(a+b+2)^2(a+b+3)} \tag{23}$$

$$= \mu_{s0}\frac{a+1}{(a+b+2)(a+b+3)} \tag{24}$$

$$= \mu_{s0}^2\frac{1-\mu_{s0}}{b+1+\mu_{s0}} \tag{25}$$

$$pdf_{s0} = \frac{(x)^{\alpha-1}(1-x)^{\beta-1}}{B(\alpha,\beta)} = \frac{(x)^b(1-x)^a}{B(b+1,a+1)} \tag{26}$$

### 3.2 General [c,d]

For the purposes of this paper, the beta distribution needs to be extended to a general interval, [c,d], e.g. $[\tau_a, \tau_b]$. To generalize these formulas, we have four parameters; two that determine the shape and two that determine the interval on which the distribution is defined. For the four parameter beta distribution, the variables $a$, $b$, $c$, and $d$ are used, where $a$ and $b$ are as before. The lower endpoint of the interval is $c$, and $d$ is the upper endpoint, so that the distribution is defined on $[c, d]$. The following equations provide formulas to compute the mean, standard deviation, and PDF on a general interval [c,d] in terms of the mean and standard deviation on [0,1]. We refer to the generalized variables with a subscript of $g$.

$$\mu_g = c + (d-c)\frac{\alpha}{\alpha+\beta} = c + (d-c)\mu_{s0} \tag{27}$$

$$\sigma_g^2 = (d-c)^2\frac{\alpha\beta}{(\alpha+\beta)^2(\alpha+\beta+1)} = (d-c)^2\sigma_{s0}^2 \tag{28}$$

Using (26) and a change of variables,

$$x = (y-c)/(d-c)$$
$$dx = 1/(b-a)dy$$

we get the following equation for the PDF

$$pdf_g = \frac{(y-c)^{\alpha-1}(d-y)^{\beta-1}}{(d-c)^{\alpha+\beta-2}B(\alpha,\beta)}\frac{1}{d-c} \tag{29}$$

$$= \frac{(y-c)^b(d-y)^a}{(d-c)^{b+a+1}B(b+1,a+1)}. \tag{30}$$

### 3.3 Standard [-1,1]

The beta distribution with support [-1,1] is also of importance in this paper. We list the following for reference.

$$\mu_{s1} = \frac{2\alpha_s}{\alpha_s+\beta_s} - 1 = \frac{\alpha_s-\beta_s}{\alpha+\beta} = \frac{b-a}{a+b+2} \tag{31}$$

$$\sigma_{s1}^2 = \frac{4\alpha_s\beta_s}{(\alpha_s+\beta_s)^2(\alpha_s+\beta_s+1)} = \frac{4(b+1)(a+1)}{(a+b+2)^2(a+b+3)} \tag{32}$$

$$pdf_{s1} = \frac{(y+1)^{\alpha-1}(1-y)^{\beta-1}}{(d+1)^{\alpha+\beta-2}B(\alpha,\beta)}\frac{1}{2} \tag{33}$$

$$= \frac{(y+1)^b(1-y)^a}{(2)^{b+a+1}B(b+1,a+1)}. \tag{34}$$

# 4 Forward Simulation

## 4.1 Orthogonal Polynomials and Jacobi Polynomials

The family of Jacobi polynomials is orthogonal with respect to the PDF for the beta distribution, (33), therefore, the Jacobi family of polynomials correspond to the beta distribution. Table 1 shows some common polynomials with the distribution they correspond to.

Table 1: Associated Distributions and Polynomials

| Distribution | Polynomial | Support |
|---|---|---|
| Gaussian | Hermite | $(-\infty, \infty)$ |
| Gamma | Laguerre | $[0, \infty)$ |
| Beta | Jacobi | $[c, d]$ |
| Uniform | Legendre | $[c, d]$ |

Every family of orthogonal polynomials has a recurrence relation, given by

$$\xi\Phi_j = a_j\Phi_{j-1} + b_j\Phi_j + c_j\Phi_{j+1}, \tag{35}$$

where $\Phi_j$ represents one of the orthogonal polynomials. The recurrence relation for Jacobi polynomials has the following coefficients,

$$a_n = \frac{2(n+\alpha)(n+\beta)}{(2n+\alpha+\beta)(2n+\alpha+\beta+1)} \tag{36a}$$

$$b_n = \frac{\beta^2 - \alpha^2}{(2n+\alpha+\beta)(2n+\alpha+\beta+2)} \tag{36b}$$

$$c_n = \frac{2(n+1)(n+\alpha+\beta+1)}{(2n+\alpha+\beta+1)(2n+\alpha+\beta+2)}. \tag{36c}$$

## 4.2 Generalized Polynomial Chaos

In order to run the inverse problem of interest, an efficient and accurate method for representing $\mathcal{P}$ at each point in space and time is needed. One option would be to use a quadrature rule on $\mathcal{P}$ and numerically integrate it over $F(\tau)$. This approach has accuracy that is polynomial ($\mathcal{O}(p^c)$). A benefit to using numerical integration is that it results in a linear combination of $p$ solutions to the Debye ODE which implies existing codes can be used to simulate, possibly in parallel. An alternate approach is to use the generalized polynomial chaos method. This method separates the time derivative from the randomness and applies a truncated expansion of $p+1$ polynomials in random space. Its accuracy can be exponential ($\mathcal{O}(c^p)$) with the right choice of polynomials. However, a downside to this approach is that it results in a linear system of ODEs. With these positives and negatives in mind, we choose to use polynomial chaos because of its fast convergence. Let us begin by expressing the random polarization in one dimension at each point in space (omitting dependence on $x$) as an expansion of orthogonal polynomials in $\xi$, such that $\tau = r\xi + m$ where $r = (d-c)/2$ and $m = (c+d)/2$.

$$\mathcal{P}(t, \xi) = \sum_{i=0}^{\infty} \alpha_i(t)\Phi_i(\xi). \tag{37}$$

where $\xi$ is a random variable with some standard distribution and $\Phi_i(\xi)$ is the $i^{th}$ orthogonal polynomial spanning our random space. In our case, $\xi \sim$Beta$(a, b)$ on [0,1], and $\Phi_i$ is a Jacobi polynomial. Therefore, we can write $\tau \sim$ Beta$(a, b)$ on the interval $[c, d]$. Plugging the expansion (37) into the equation (19) results in

$$(r\xi + m)\sum_{i=0}^{\infty} \dot{\alpha}_i(t)\Phi_i(\xi) + \sum_{i=0}^{\infty} \alpha_i(t)\Phi_i(\xi) = \varepsilon_0\varepsilon_d E. \tag{38}$$

Using the recurrence relation and projecting onto the finite dimensional random space spanned by $\{\Phi_j\}_{j=0}^p$, we get

$$\begin{aligned} r\sum_{i=0}^{p}\dot{\alpha_i}(t)\left[a_i\langle\Phi_{i+1},\Phi_j\rangle_w + b_i\langle\Phi_i,\Phi_j\rangle_w + c_i\langle\Phi_{i-1},\Phi_j\rangle_w\right] \\ +\sum_{i=0}^{p}\left[\alpha_i(t)+m\dot{\alpha_i}(t)\right]\langle\Phi_i,\Phi_j\rangle_w = \varepsilon_0\varepsilon_d E\langle\Phi_0,\Phi_j\rangle_w \end{aligned} \tag{39}$$

where $\langle\Phi_i,\Phi_j\rangle_w$ is the weighted inner product of $\Phi_i$ and $\Phi_j$, with weighting function, $w$, corresponding to the Beta distribution. We denote the $p+1$ truncation of $\{\alpha_i\}_{i=0}^{\infty}$ by $\vec{\alpha}$. Using the orthogonality of the polynomials with the distribution (details provided in [5]), we simplify this to

$$(rM+mI)\dot{\vec{\alpha}}+\vec{\alpha}=\varepsilon_0\varepsilon_d E\vec{e_1}$$

$$M=\begin{bmatrix} b_0 & a_1 & & & \\ c_0 & b_1 & a_2 & & \\ & \ddots & \ddots & \ddots & \\ & & \ddots & \ddots & a_p \\ & & & c_{p-1} & b_p \end{bmatrix}.$$

The entries of Jacobi matrix $M$ are the coefficients of the recurrence relation defined in (36) Let us denote this system by

$$A\dot{\vec{\alpha}}+\vec{\alpha}=\vec{f}. \tag{40}$$

Note that $\vec{f}$ is dependent on the electric field, which is dependent on the expected value of the random polarization, $\mathrm{E}[\mathcal{P}]$. It can be shown that the macroscopic polarization, $P(t,x;F)=\mathrm{E}[\mathcal{P}]=\alpha_0(t,x)$ [12].

### 4.3 Discretization

We now have the following model for the forward problem. The first two equations come from Maxwell's equations (with $P$ replaced by $\alpha_0$). We get the third equation from the generalized polynomial chaos approximation of the polarization.

$$\varepsilon\frac{\partial E}{\partial t}=-\frac{\partial H}{\partial x}-\sigma E-\frac{\partial\alpha_0}{\partial t} \tag{41a}$$

$$\frac{\partial H}{\partial t}=-\frac{1}{\mu_0}\frac{\partial E}{\partial x} \tag{41b}$$

$$A\dot{\vec{\alpha}}+\vec{\alpha}=\vec{f} \tag{41c}$$

where

$$f=\epsilon_0(\epsilon_s-\epsilon_\infty)E\hat{e_1}. \tag{42}$$

We interrogate the medium surrounded by a vacuum. The source signal is emitted on one side of the medium, and the receiver is placed on the opposite side. The receiver measures the electric field after it has passed through the medium. We scale the domain to be between zero and one and to truncate the computational domain, we use the absorbing boundary conditions,

$$[\dot{E}-c_0E']_{x=0}=[\dot{E}+cE']_{x=1}=0 \tag{43}$$

where $c_0$ is the speed of light in a vacuum. We assume no sources are present aside from the interrogating signal, so initial conditions are

$$E(0,x)=0$$
$$\dot{E}(0,x)=0.$$

For our discretization, we use a modified Yee Scheme on (41) and (41b) along with Crank-Nicolson on (41c). The standard Yee Scheme [13] is frequently used in electromagnetic problems involving Maxwell's equations in dielectrics. This modified scheme uses a staggered grid such that $E$ and $\alpha_0$ have half steps in time and integer steps in space, and $H$ has half steps in space and integer steps in time. It is an explicit second order scheme in space and time, which is conditionally stable if the CFL condition is satisfied. The CFL condition is

$$\nu = \frac{c\Delta t}{\Delta x} \leq 1 \tag{44}$$

where $c = 1/\sqrt{\epsilon\mu}$. We let $n$ represent the time step and $k$ represent the space step,

$$\frac{E_k^{n+\frac{1}{2}} - E_k^{n-\frac{1}{2}}}{\Delta t} = -\frac{1}{\epsilon}\frac{H_{k+\frac{1}{2}}^n - H_{k-\frac{1}{2}}^n}{\Delta x} - \frac{1}{\epsilon}\frac{\alpha_{0_k}^{n+\frac{1}{2}} - \alpha_{0_k}^{n-\frac{1}{2}}}{\Delta t} \tag{45a}$$

$$\frac{H_{k+\frac{1}{2}}^{n+1} - H_{k+\frac{1}{2}}^n}{\Delta t} = -\frac{1}{\mu}\frac{E_{k+1}^{n+\frac{1}{2}} - E_k^{n+\frac{1}{2}}}{\Delta x} \tag{45b}$$

$$A\frac{\vec{\alpha}_k^{n+\frac{1}{2}} - \vec{\alpha}_k^{n-\frac{1}{2}}}{\Delta t} + \frac{\vec{\alpha}_k^{n+\frac{1}{2}} + \vec{\alpha}_k^{n-\frac{1}{2}}}{2} = \frac{\vec{f}^{n+\frac{1}{2}} + \vec{f}^{n-\frac{1}{2}}}{2} \tag{45c}$$

where $f$ is given in (42). It was shown in [5] that (44) holds for (45) when $p = 2$. We discretize the boundary conditions to be

$$E_0^{n+1} = (1-\nu)E_0^n + \nu E_1^n \tag{46}$$

$$E_K^{n+1} = (1-\nu)E_K^n + \nu E_{K-1}^n. \tag{47}$$

# 5 Time-Domain Inverse Problem Formulation

## 5.1 Inverse Problem for Distributions

Let $E(t_j, x_i; F)$ represent the simulated electric field using probability measure, $F$. Given $N$ data points $\{\hat{E}_j\}_{j=1}^N$ measured at a receiver location, $x_r$ (which we assume to be a node in our spatial discretization), we have the cost function,

$$\mathcal{J}(F) = \frac{1}{N}\sum_j \left(E(t_j, x_r; F) - \hat{E}_j\right)^2. \tag{48}$$

We seek to determine a probability measure $F^*$, such that

$$F^* = \min_{F\in\mathfrak{P}(\mathcal{N})} \mathcal{J}(F),$$

A minimum of $\mathcal{J}(F)$ over $\mathfrak{P}(\mathcal{N})$ is shown to exist in [3] when $P$ is given by (18). It is important for the forward simulation to be efficient and accurate since for each iteration of the inverse problem it is evaluated.

## 5.2 Inverse Problem Setup

The probability measure is assumed to be a Beta distribution, which we parameterize by its mean, $\mu$, and standard deviation, $\sigma$. Using MATLAB's non linear least squares solver with the Levenberg-Marquardt algorithm, we run the inverse problem to find the distribution of relaxation times. There are three different problems we consider, in all but one case of the last problem, we attempt to recover a single beta distribution.

(i) "Usual"

(ii) Debye

(iii) Multi-pole

Problem i runs the inverse problem on a "usual" beta distribution of relaxation times. "Usual" refers to the downward facing curved distributional shape with finite support. Problem ii runs the inverse problem for the "distribution" where the relaxation time is a scalar. This would correspond to a delta-like distribution. Problem iii runs the problem using a linear combination of two "usual" beta distributions. Here we expect to recover some average of two beta distributions.

### 5.3 Synthetic Data for Beta Distribution

In lieu of real data, we synthesize our data using the methods described in this section. For Problems i and iii (i.e., not Debye), we synthesize data using the forward simulation with a refined time step and with $p = 8$, then add mean zero, constant variance noise. We assume the relaxation times follow a beta distribution on a fixed interval, $[c, d]$. The "actual" beta distribution uses $a = 5$, $b = 2$, which yields a mean of $1/3$ and standard deviation of about 0.1491 on the standard interval $[0, 1]$. The forward simulation uses $p = 8$ for the polynomial chaos system to ensure that it is fully converged. For Problem (ii), we synthesize data using a different forward simulation than is used in the inverse problem. In this case, we use $p = 0$ to synthesize the data and add mean zero, constant variance noise, but use $p = 8$ in the forward solve to recover $\tau$. By setting $p = 0$, we force the relaxation time to be a scalar value. The "actual" relaxation time here is $1/3$ on the standard interval $[0, 1]$.

### 5.4 Source signal

A windowed sine wave of frequency 10GHz and a UWB pulse with frequencies ranging from $10^8$ to $10^{10}$Hz are used. These are two separate experiments, the UWB is more like what is done in practice. The UWB pulse is defined as

$$\sum_{i=1}^{n} \varphi_i \sin(2\pi\phi_i(t)) \tag{49}$$

where $\phi_i$ is linearly spaced from $10^8$ to $10^{10}$, and $\varphi_i$ is defined by the beta distribution with $a = 4$, $b = 1$. By considering a range of frequencies, we hope to excite more than one pole in the dielectric.

### 5.5 Levenberg Marquardt

Given an initial guess for the mean, $\mu_0$, and standard deviation, $\sigma_0$ of the distribution of relaxation times, the Levenberg-Marquardt algorithm uses a combination of Gauss-Newton and Steepest Descent methods to find the minimizer of (48). When the Levenberg-Marquardt parameter $\lambda$ is large, the algorithm acts more like the Steepest Descent method. When $\lambda$ is small, it acts more like Gauss Newton. It is an iterative method which begins with an initial guess, increases and/or decreases the parameters and computes the cost function at each iteration. The cost function, $\mathcal{J}(F)$, should exhibit sufficient decrease at each iteration, as this would imply the parameters are converging to those of the actual distribution. The Levenberg-Marquardt algorithm is an option within the `lsqnonlin` function in MATLAB. The details that we give `lsqnonlin` are:

- Function Tolerance: $10^{-11}$
- Step Tolerance: $10^{-10}$
- Initial (Levenberg-Marquardt) Regularization Parameter ($\lambda$): 1000

The confidence intervals shown in this paper are produced from taking the square root of the diagonal elements of the covariance matrix, which is given by the algorithm and is computed using the approximate derivatives of the function with respect to the parameters.

### 5.6 Initial Guess

For Problem i and ii, the domain of the beta distribution in terms of its parameters $\mu_s$ and $\sigma_s$ on the interval $[1.355 \times 10^{-12}, 2.168 \times 10^{-11}]$ is shown in Figure 4.

We scale the domain to $\mu_s \in$ [0,1]. The maximum standard deviation in the standard domain can be found

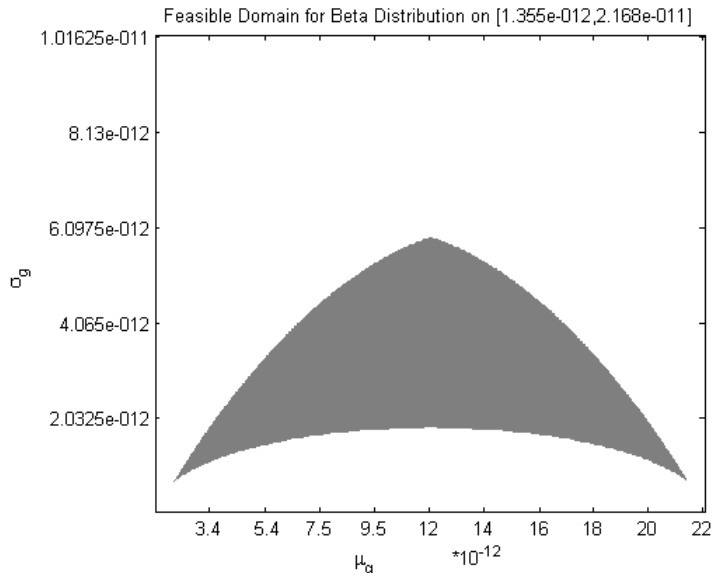


Figure 4: Feasible Domain for Beta Distribution on [$1.355e^{-12}$,$2.168e^{-11}$]

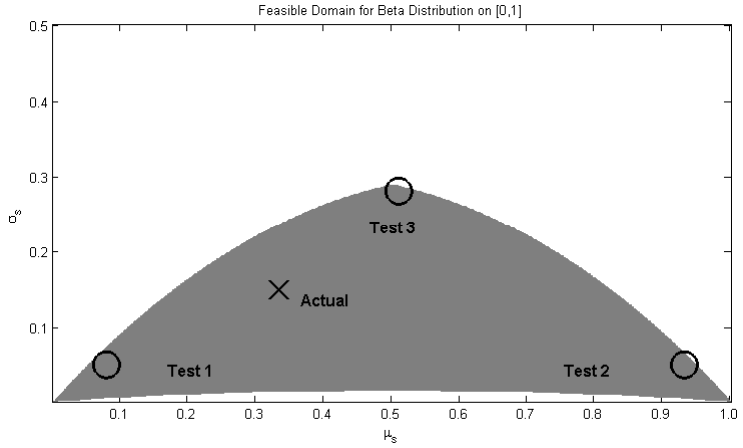


Figure 5: Feasible Domain for Beta Distribution on [0,1]

to be $1/\sqrt{12}$ using the formulas given in Sections 3.1. We test the inverse problem for the distribution with three different initial guesses for Problems i and ii at the three "corners" of the domain. These tests, Test 1, Test 2 and Test 3, refer to their corresponding initial guesses in Figure 5. In Section 6 for each of the three initial guesses, we run the inverse problem with mean zero, constant variance noise with noise level examples 0, 0.05, and 0.1. Because of the iterative nature of the algorithm, we are able to show the iteration histories. Also, 95% confidence intervals are produced and plotted with the estimates versus the noise level. Confidence intervals give a measure of how sure we can be of our optimal solution. The smaller the intervals are, the more confident we can be.

# 6 Results

This section contains the results from the three Problems described in Section 5.2. Within each Problem, there are two interrogating pulses. Within each pulse section, there are plots of the electric field data and the beta distributions for the highest noise level and all three initial tests. The figures for the iteration histories and 95% confidence intervals are included in Appendices A and B. The smaller the bars are in the confidence intervals, the more sure we can be in our optimal solution. The figures of the electric field data each have four curves. These curves correspond to the synthetic data, the "Initial" field, the "Optimal" field, and the "Actual" field. We describe how the synthetic data is generated in Section 5.3. The "Initial" curve is computed by running the forward simulation with the initial guess. The "Optimal" curve is computed by running the forward simulation using the distribution returned from the inverse problem. The "Actual" curve is computed by running the forward simulation with no noise or refinement with the actual distribution. The caption and title for each of the plots give information about the details of what is shown. The noise level, refinement, test, and pulse information is provided. Note that the noise level 0.1 is the highest noise level we used. We use a truncated sine wave pulse as well as a UWB pulse.

## 6.1 Problem i: Usual Distribution

The "Actual" distribution for this Problem has a mean of 1/3 and a standard deviation of approximately 0.1491. Each test is represented by two figures in this section; one of the electric field and one of the distributions.

### 6.1.1 Windowed Sine Wave

The electric fields for each of the initial tests are shown in Figures 6, 8, 10. The distributions for each of the initial tests are shown in Figures 7, 9, 11. In each of the figures in this section, note that the"Optimal" electric field is much closer to the data curve, and the "Optimal" distribution is much closer to the "Actual" than the "Initial". The figures are qualitatively convincing that the inverse problem works as intended.

Appendix A shows the 95% confidence intervals and iteration history figures. The 95% confidence intervals give mathematical validation that the method is finding the right distribution. The iteration histories give insight into what the algorithm is doing at each iteration. The confidence intervals show that we can be 95% confident that the distributions shown in this section are the correct distributions. Figures 27 through 30 show that we can be confident of our results. The confidence intervals are plotted against the noise level and the intervals increase as the noise increases. Notice that the intervals in the confidence interval plots are relatively small, so we can be 95% sure the optimal solution is a good one. For example, the confidence interval for the mean of the distribution of relaxation times for Problem i is shown in Figure 12.

In Appendix A, Figures 31, 33, and 35 show the iteration histories for the windowed sine pulse at each of the three initial points. An 'x' is placed at the actual value, and the plots show the path the algorithm took to get there. Figures 32, 34, and 36 show the iteration histories using the UWB pulse. Notice that the inverse problem does not always take the shortest path to the actual solution. However, it finds the solution we are trying to determine. In particular, this solution method determines the mean value first and then attempts to resolve variance.

### 6.1.2 UWB Pulse

The plots in this section are created with the UWB pulse as the interrogating signal. The electric field is shown in Figures 13, 15, and 17. The beta distribution is shown in Figures 14, 16, and 18. The figures imply that the electric fields and distributions are converging. The confidence intervals and iteration histories are shown in Appendix A and verify that we can be confident with our findings.

## 6.2 Problem ii: Debye

For this Problem, the relaxation time is defined to be a scalar ($\tau = 1/3$), instead of a distribution as in Problem i. As discussed in Section 5.3, the data for this Problem is synthesized with a different simulation than is used to recover the relaxation time in the inverse problem. The simulation used to recover the

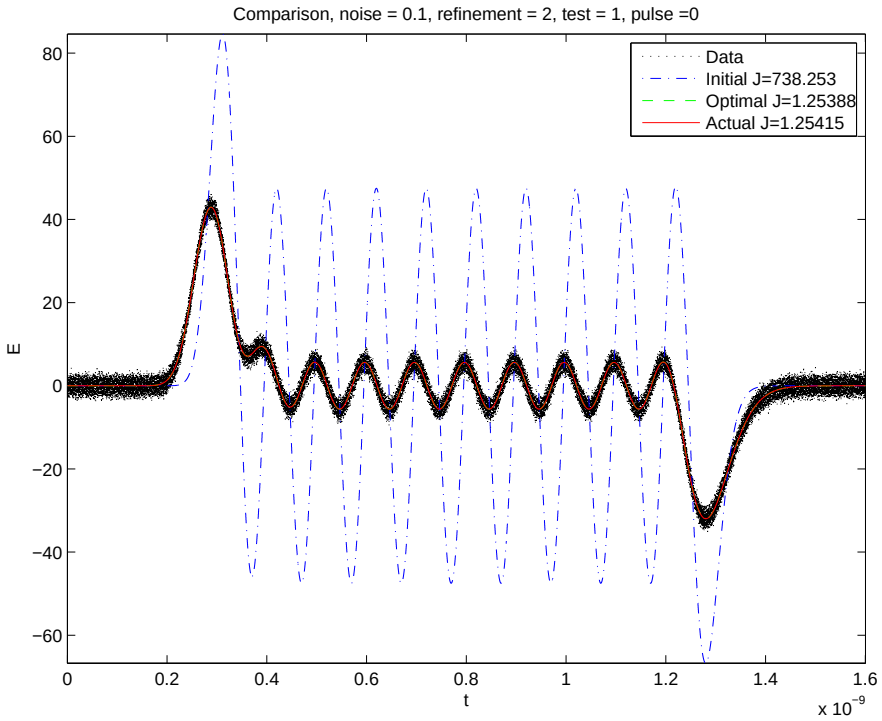


Figure 6: Comparison of Results to Data using Noise Level 0.1, Refinement of 2, Test 1, Truncated Sine Wave

relaxation time assumes it follows a distribution, while the generated data uses a scalar. Although $\tau$ is a scalar, it can be thought of as a delta distribution.

The inverse problem, recall, is limited to changing the mean and standard deviation. Therefore, one might assume the optimal distribution would have a mean of $\tau$ and a standard deviation of zero, or $\varepsilon_{\texttt{mach}}$. This would make sense, however, as we see, it is not the case. The inverse problem recovers a mean of 0.335, and a standard deviation of 0.052. This can be explained by the different simulations being used. It is reasonable not to expect to get the exact relaxation time back from the inverse problem when we use a completely different method to synthesize the data. It is important to note, however, that the optimal mean is close to the actual.

In this Problem, unlike in Problem i, the "Actual" distribution is a delta distribution, and is represented by a vertical line at its mean. We also plot the optimal distribution in the form of a vertical line, as its variance is too small to be plotted. As can be seen in the figures, the initial distribution we start with is a "usual" beta distribution (as in Problem i). By computing a coarse surface plot of the cost function with varying mean and standard deviation (not shown), we determine that in fact, the minimum occurs when the mean is 0.335 instead of at 1/3 and standard deviation is 0.05 instead of 0. The minimum is not where we expect, however, the inverse problem recovers the correct minimum. The confidence intervals and iteration histories are shown in Appendix B.

Appendix B includes 95% confidence intervals and iteration histories for the mean and standard deviation of the distributions found in Problem ii. Figures 37 through 40 show the confidence intervals and Figures 43 through 46 show the iteration history for each of the initial tests. Recall in this problem we expect the optimal solution to have mean 1/3 and standard deviation of zero. The 'x' in the iteration histories plots marks the expected optimal solution. Notice that instead, the iterations end at around a mean of 0.335 and standard deviation of 0.05. So, it is clear that the results for Problem ii are not as good as the results for Problem i.

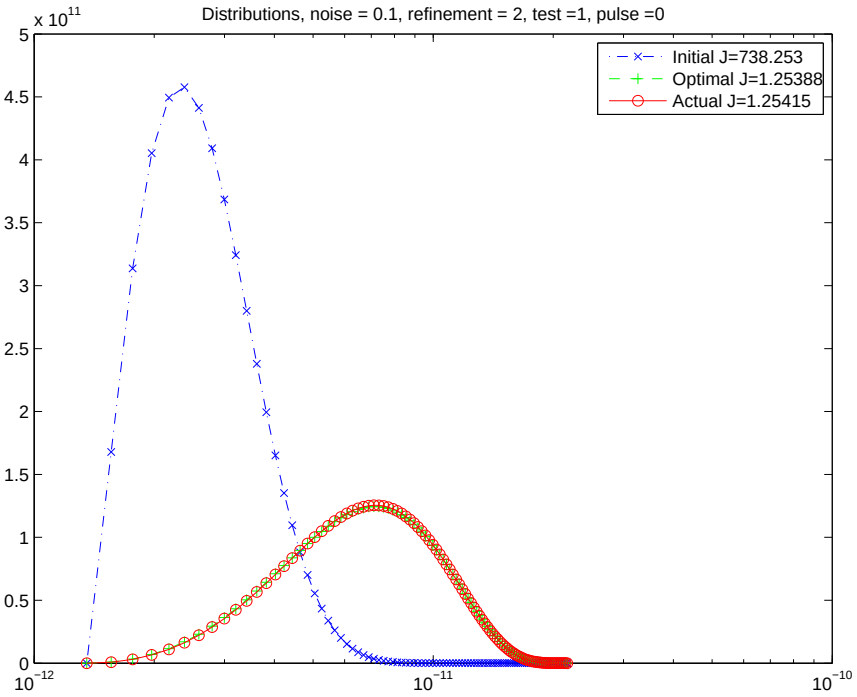


Figure 7: Comparison of Results to the Distribution using Noise Level 0.1, Refinement of 2, Test 1, Truncated Sine Wave

### 6.2.1 Windowed Sine Wave

The electric field figures for the Debye case are omitted. This is because they are qualitatively the same as in Problem i. The distributions are shown in Figures 19, 20, and 21. Since the forward simulator for the actual data is different than the forward simulator used in the inverse problem, this is acceptable. It is reasonable to find a different optimal distribution than the actual, especially when the cost function is smaller in the optimal case than the actual.

### 6.2.2 UWB Pulse

Testing the Debye case with the UWB pulse yields the same results as the windowed sine wave. The electric field for the three tests are omitted, as before. The distributions are shown in Figures 22, 23, and 24. Although the optimal mean is closer to the actual mean than the initial mean, the distribution has not converged to the exact.

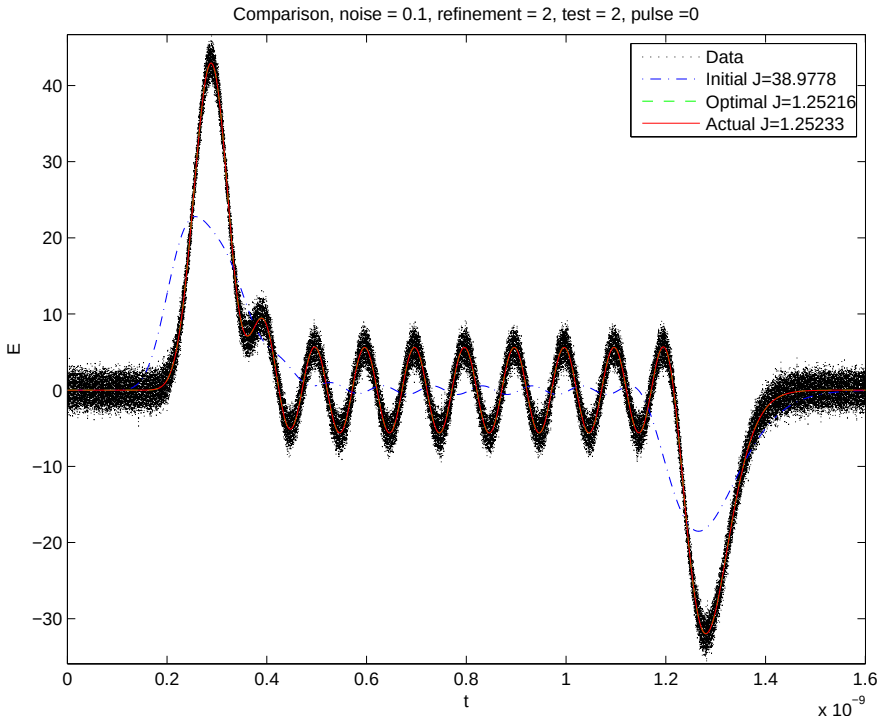


Figure 8: Comparison of Results to Data using Noise Level 0.1, Refinement of 2, Test 2, Truncated Sine Wave

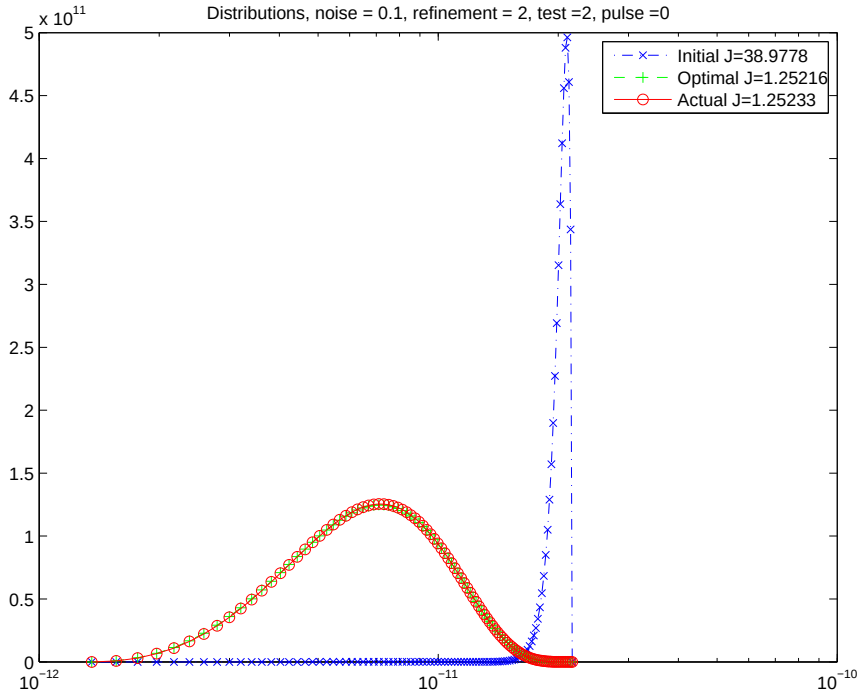


Figure 9: Comparison of Results to the Distribution using Noise Level 0.1, Refinement of 2, Test 2, Truncated Sine Wave

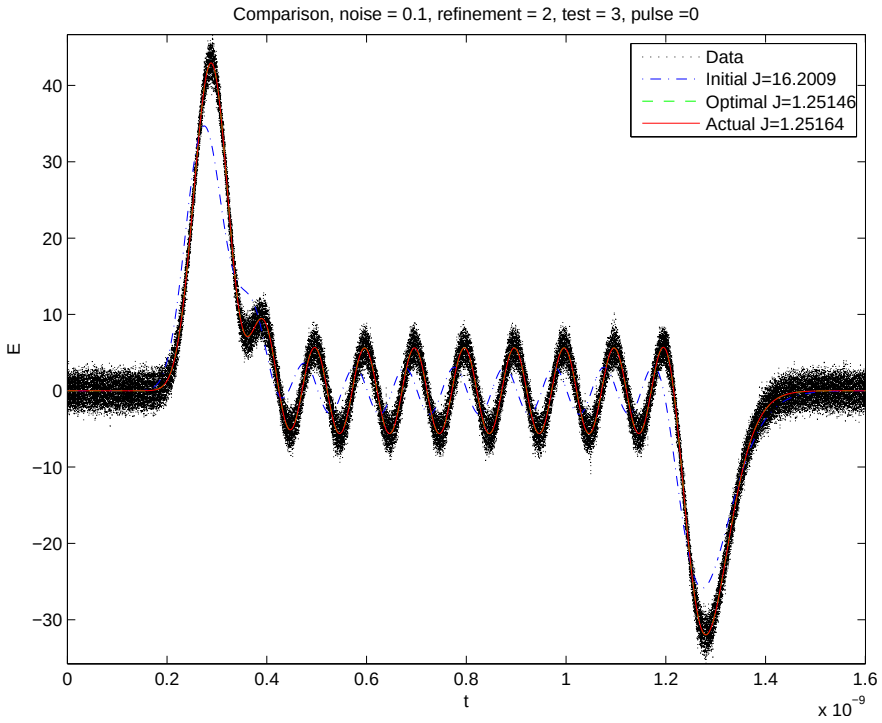


Figure 10: Comparison of Results to Data using Noise Level 0.1, Refinement of 2, Test 3, Truncated Sine Wave

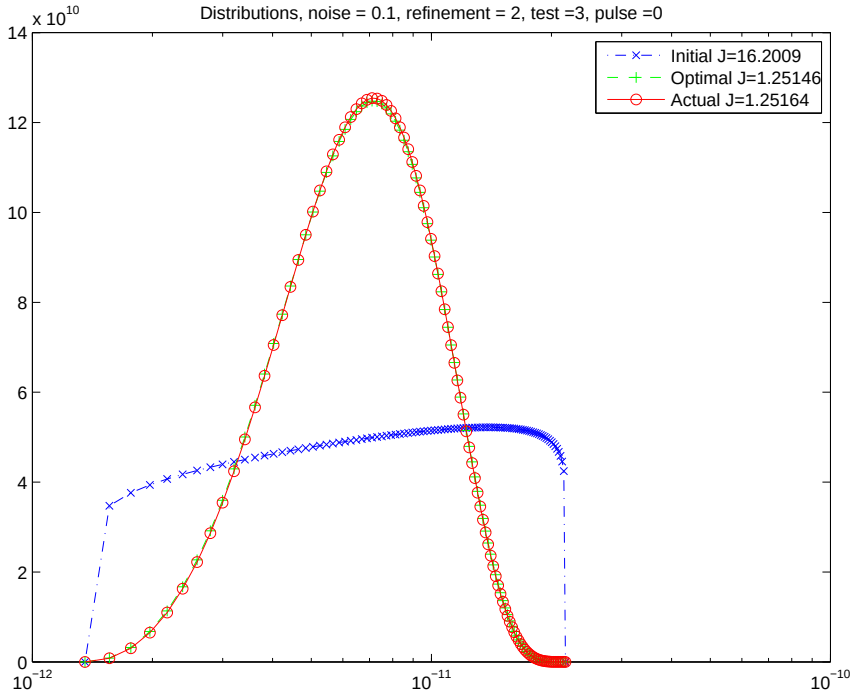


Figure 11: Comparison of Results to the Distribution using Noise Level 0.1, Refinement of 2, Test 3, Truncated Sine Wave

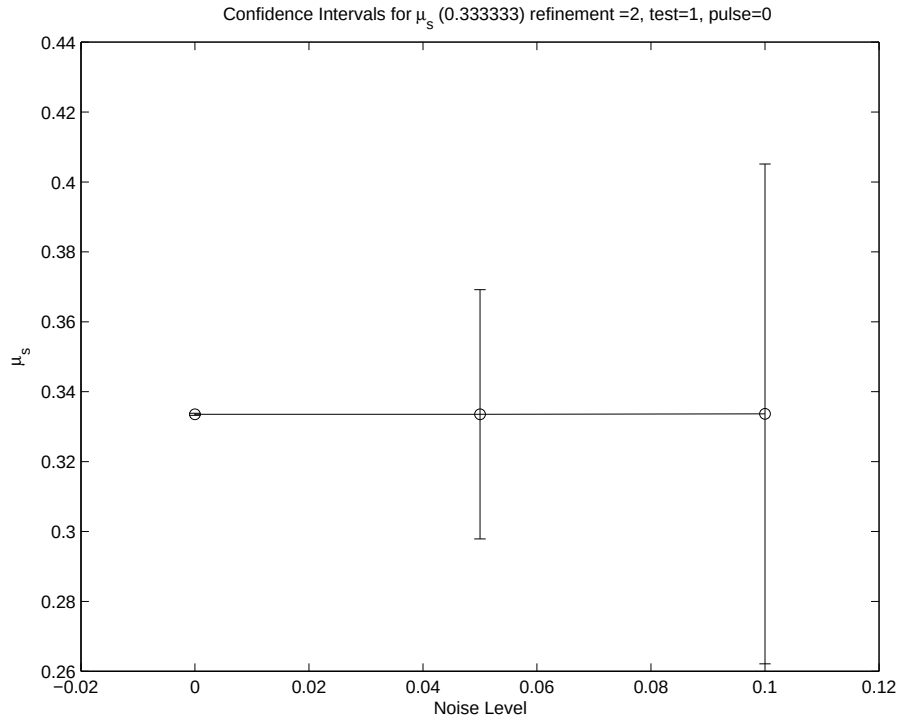


Figure 12: Estimate of Mean using Refinement of 2 and Truncated Sine Wave

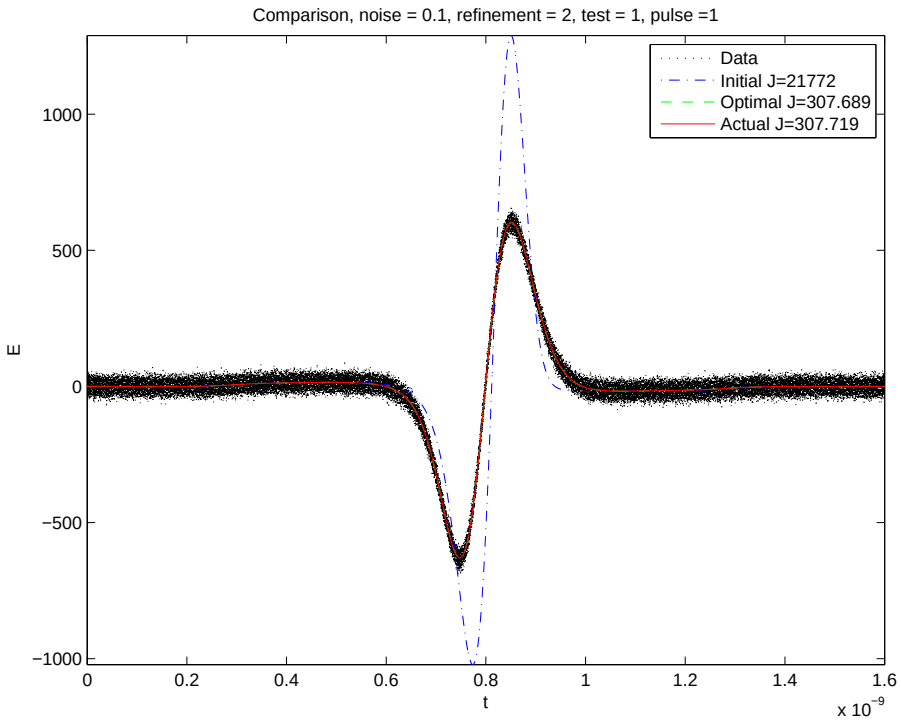


Figure 13: Comparison of Results to Data using Noise Level 0.1, Refinement of 2, Test 1, UWB Pulse

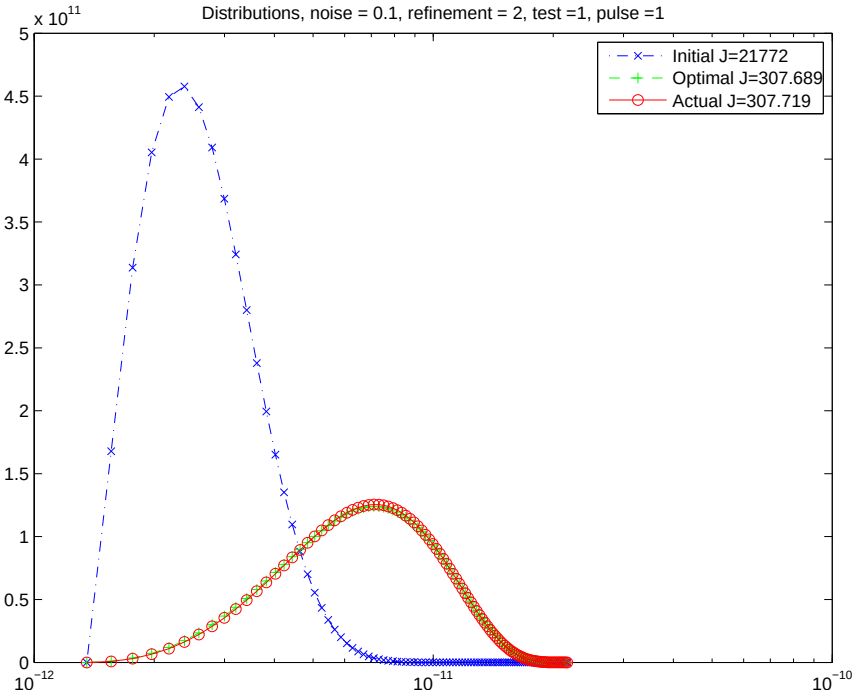


Figure 14: Comparison of Results to the Distribution using Noise Level 0.1, Refinement of 2, Test 1, UWB Pulse

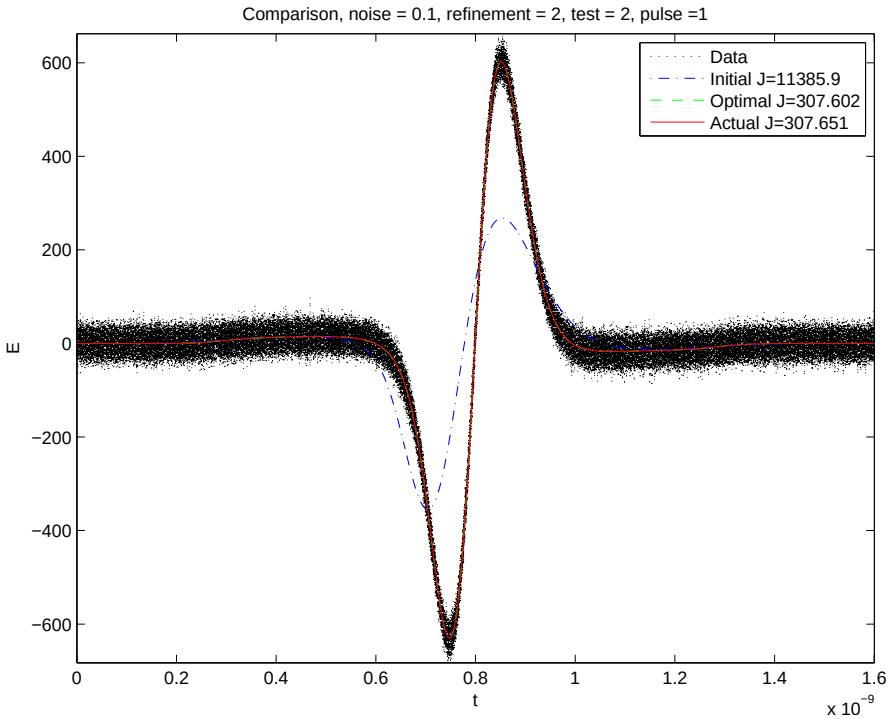


Figure 15: Comparison of Results to Data using Noise Level 0.1, Refinement of 2, Test 2, UWB Pulse

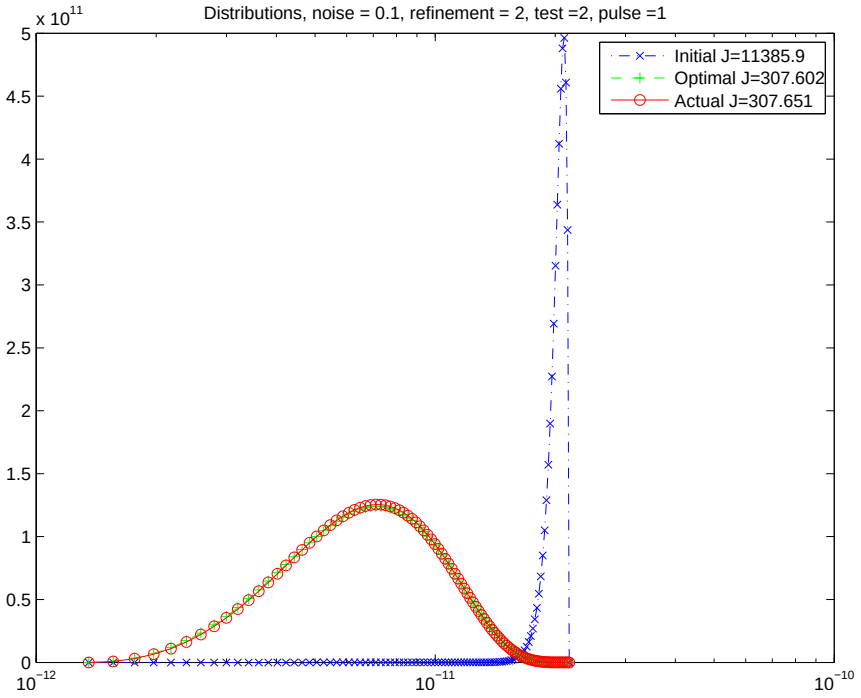


Figure 16: Comparison of Results to the Distribution using Noise Level 0.1, Refinement of 2, Test 2, UWB Pulse

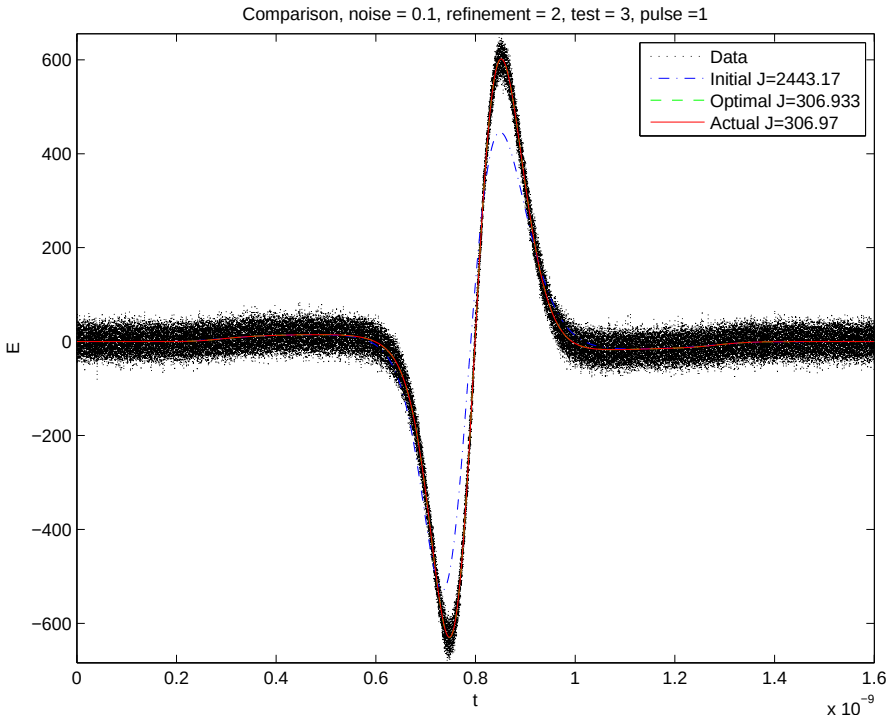


Figure 17: Comparison of Results to Data using Noise Level 0.1, Refinement of 2, Test 3, UWB Pulse

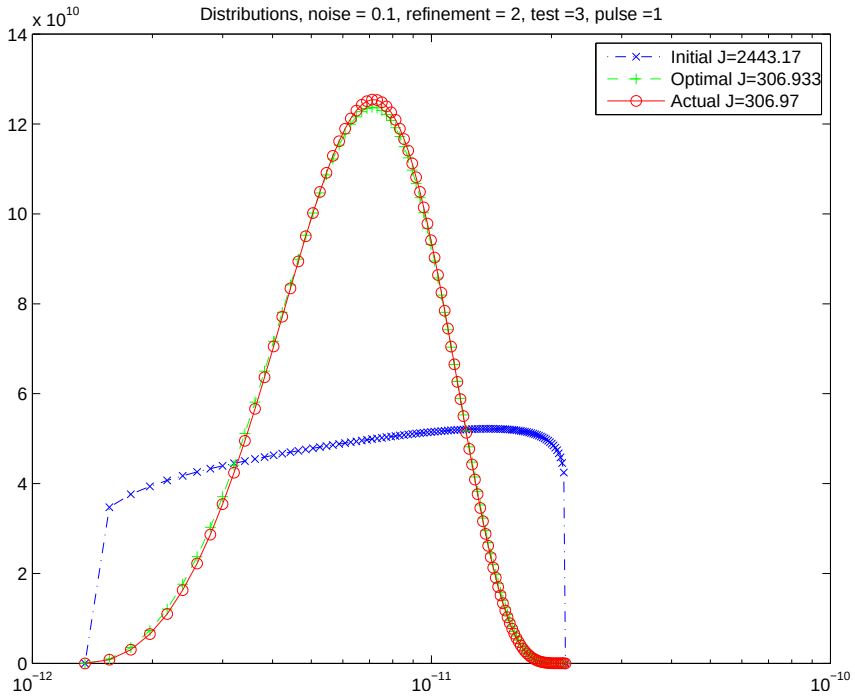


Figure 18: Comparison of Results to the Distribution using Noise Level 0.1, Refinement of 2, Test 3, UWB Pulse

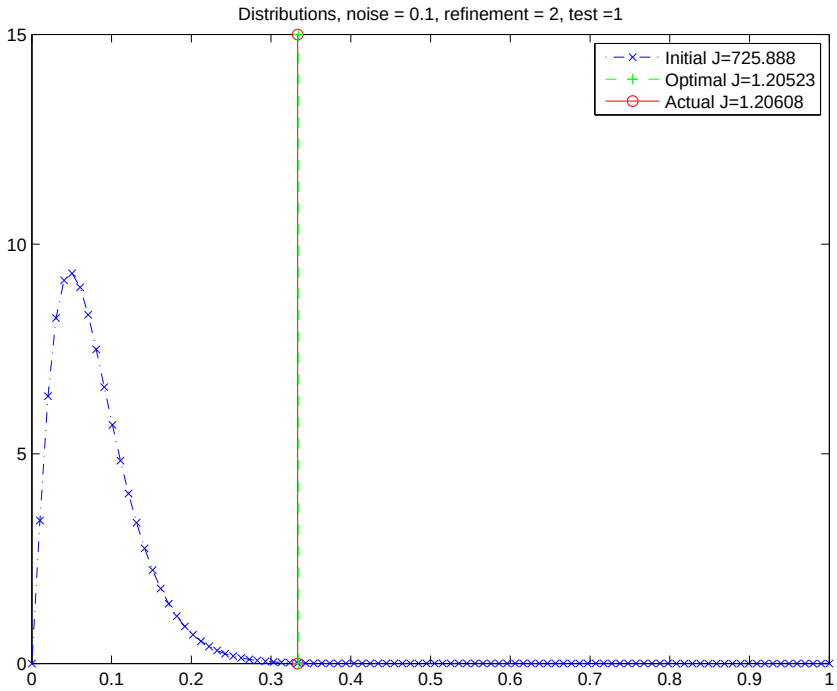


Figure 19: Comparison of Debye Results to the Distribution using Noise Level 0.1, Refinement of 2, Test 1, Truncated Sine Wave

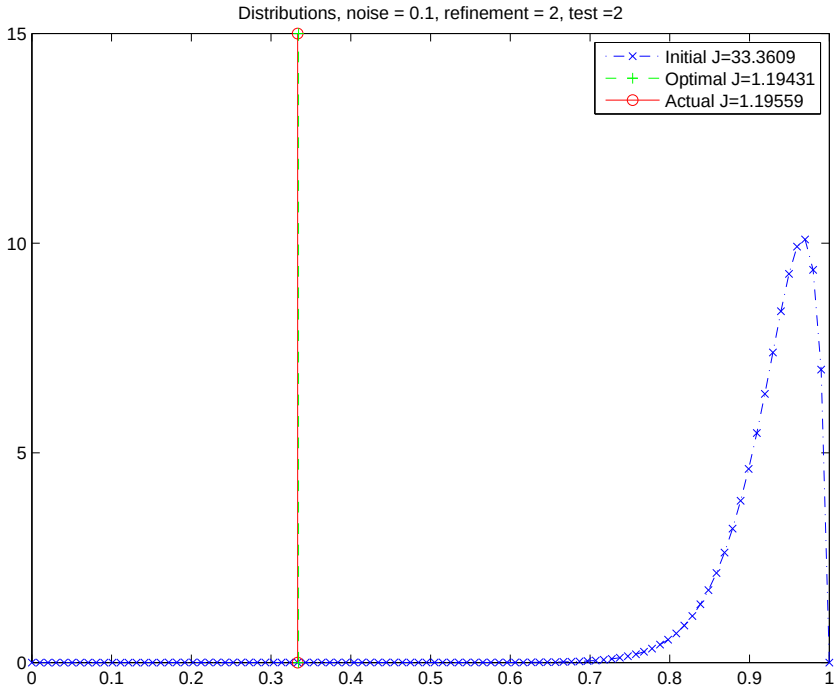


Figure 20: Comparison of Debye Results to the Distribution using Noise Level 0.1, Refinement of 2, Test 2, Truncated Sine Wave

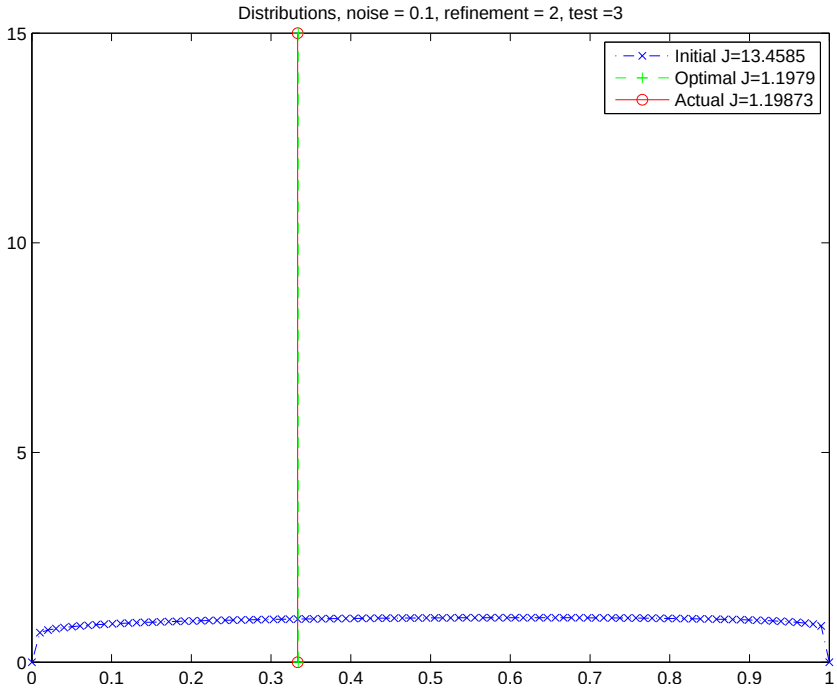


Figure 21: Comparison of Debye Results to the Distribution using Noise Level 0.1, Refinement of 2, Test 3, Truncated Sine Wave

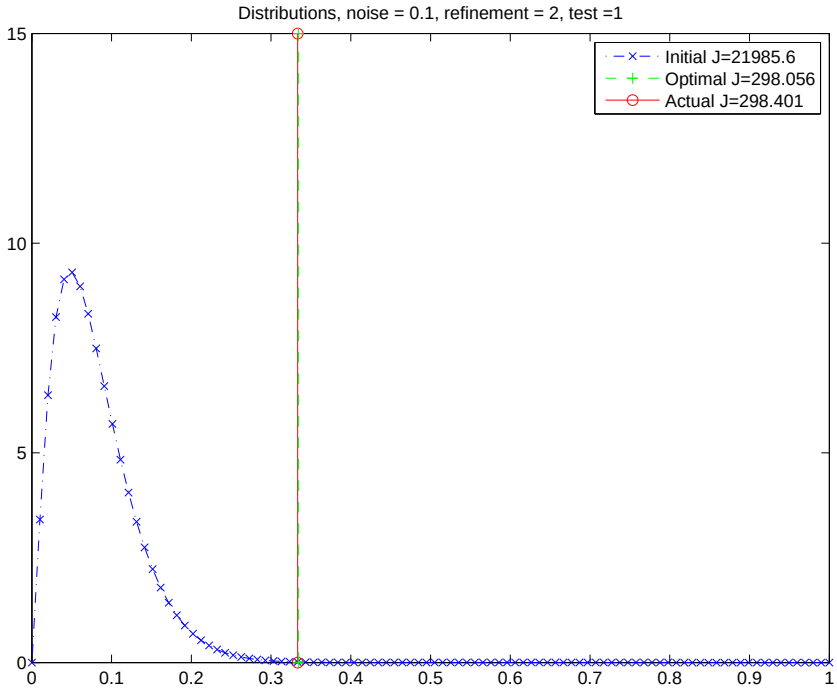


Figure 22: Comparison of Debye Results to the Distribution using Noise Level 0.1, Refinement of 2, Test 1, UWB Pulse

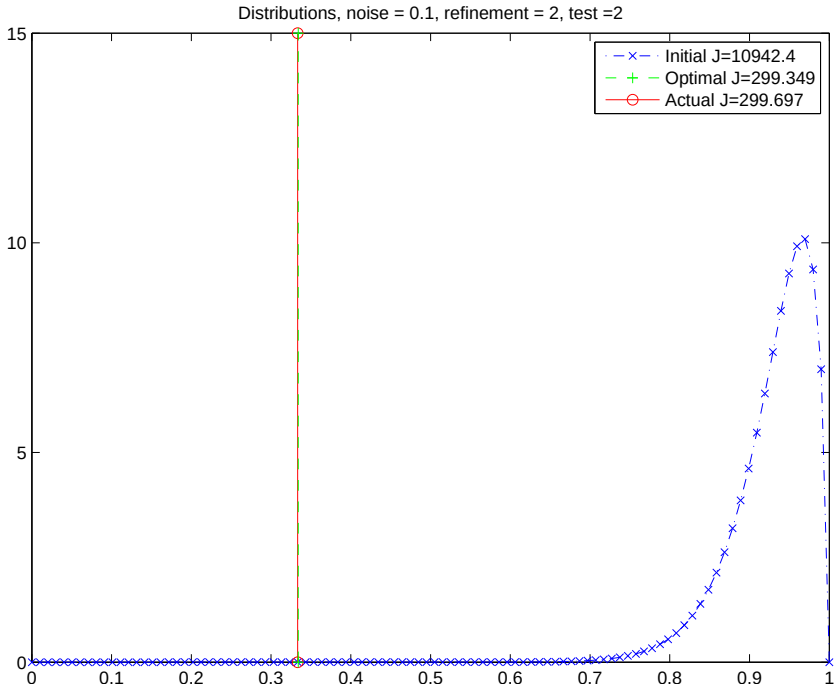


Figure 23: Comparison of Debye Results to the Distribution using Noise Level 0.1, Refinement of 2, Test 2, UWB Pulse

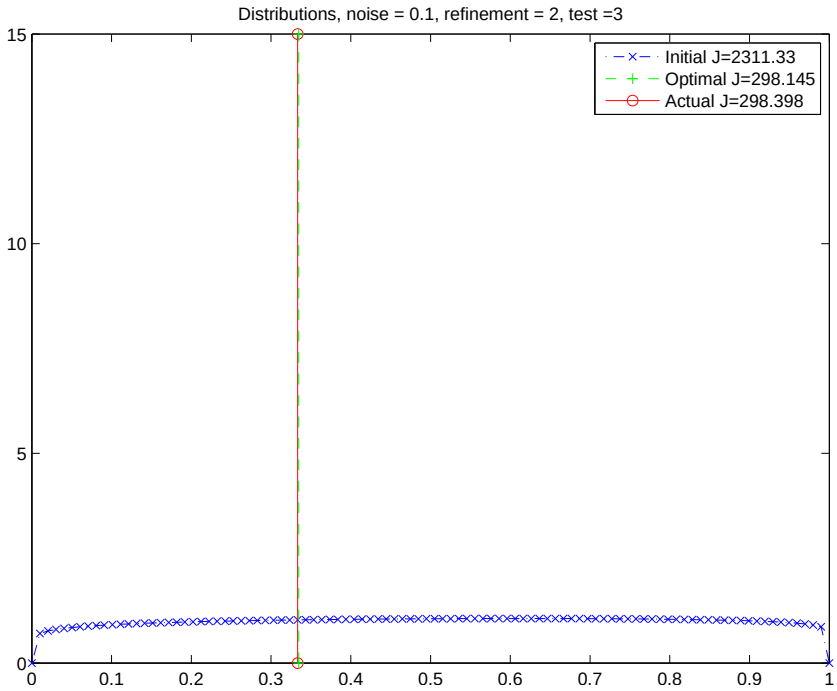


Figure 24: Comparison of Debye Results to the Distribution using Noise Level 0.1, Refinement of 2, Test 3, UWB Pulse

## 6.3 Problem iii: Multi-pole

Dispersive dielectrics are typically composed of multiple materials. Each of these materials has a distribution of relaxation times. It is not always possible to isolate each material to test it and find the distribution of relaxation times (as in Problem i). The development of our forward model for one distribution easily extends to two distributions. We extend (16), to two distributions, $F_1$ and $F_2$, represented by $\tau_1$, $\tau_2$, two polarizations, $P_1$, $P_2$, which have parameters $\varepsilon_{d1}$, $\varepsilon_{d2}$. They are related in the following way

$$\tau_1 \dot{P}_1 + P_1 = \varepsilon_0 \varepsilon_{d1} E \tag{50}$$

$$\tau_2 \dot{P}_2 + P_2 = \varepsilon_0 \varepsilon_{d2} E \tag{51}$$

and

$$\varepsilon(\omega) = \varepsilon_0 \varepsilon_\infty + \frac{\varepsilon_0 \varepsilon_{d1}}{1 + i\omega\tau_1} + \frac{\varepsilon_0 \varepsilon_{d2}}{1 + i\omega\tau_2}. \tag{52}$$

The distribution we are modeling is a bi-modal distribution given by

$$F = \varepsilon_{d1}/\varepsilon_d F_1 + \varepsilon_{d2}/\varepsilon_d F_2 \tag{53}$$

where $\varepsilon_d = \varepsilon_{d1} + \varepsilon_{d2}$. So, we can think of $\varepsilon_{d1}/\varepsilon_d$ as a weight, $\gamma$. In this case, $\varepsilon_{d2}/\varepsilon_d$ is $1 - \gamma$. This ensures $F$ still integrates to one. We run two tests on the multi-pole version of the inverse problem. Test 4 uses simulated data with two distributions of relaxation times. In this test, the initial guess is a single distribution. The inverse problem tries to recover a single distribution, while the data comes from multiple distributions. This is applicable to reality, in the sense that the material of interest might have two materials in it, but the experimenter may not know that. Also, in this experiment the inverse problem does a two parameter search. The results for the distribution for this test with a noise level of 0.1 and a refinement of 2 are shown in Figure 25. The initial guess is at one of the two actual distributions. It seems as if the optimal distribution tries to fit one of the poles of the actual distribution more so than the other.

Test 5 uses simulated data with two distributions of relaxation times. The inverse problem searches for two distributions. The optimization routine is given two initial distributions and does a four parameter search for the solution($F_1$ and $F_2$ assuming $\gamma$ given). The distribution results for this test with noise level of 0.1 and a refinement of 1 are shown in Figure 26. The initial guess, as can be seen is a bimodal distribution. The optimal solution is plotted as a vertical line at the mean. The actual mean is also shown as a vertical line for reference. The inverse problem seems to find the mean values of the distributions, and makes the standard deviations very small. This would imply that the mean values of the distributions are the most important factors to the electric field data. This is consistent with the numerical results in [2] when there is limited data.

Test 5 gives a better qualitative approximation to the actual distribution by finding approximate mean values. Notice that in both of the tests within Problem iii, the inverse problem does not work as well as in Problem i. The electric field data fits well in both tests (4 and 5), however, the distributions are not as close of a match.

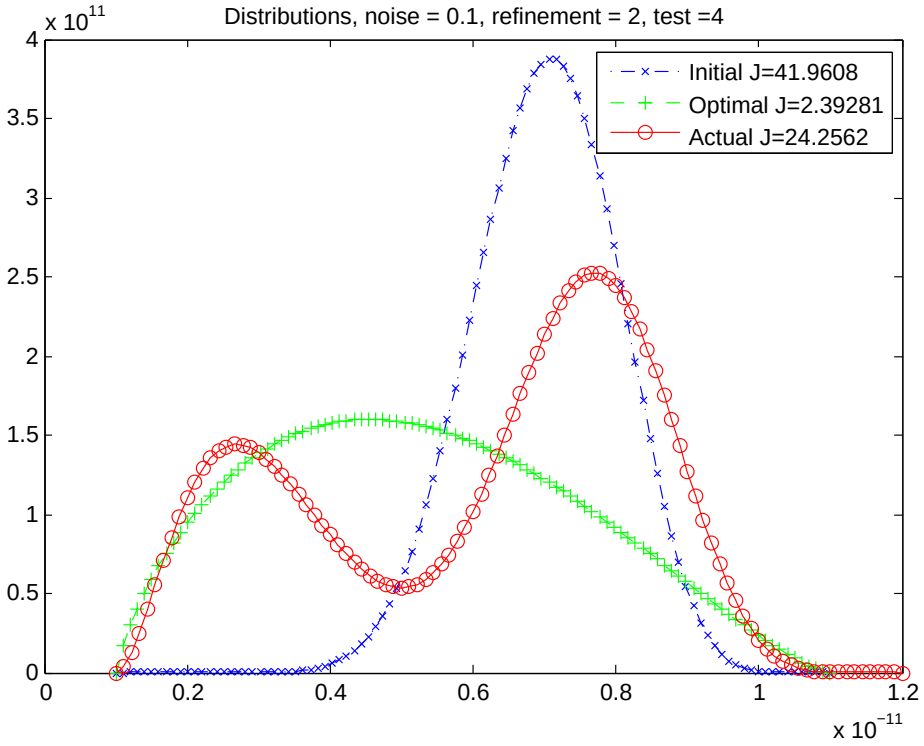


Figure 25: Comparison of Multi-Pole Results to the Distribution using Noise Level 0.1, Refinement of 2, Test 4, Truncated Sine Wave

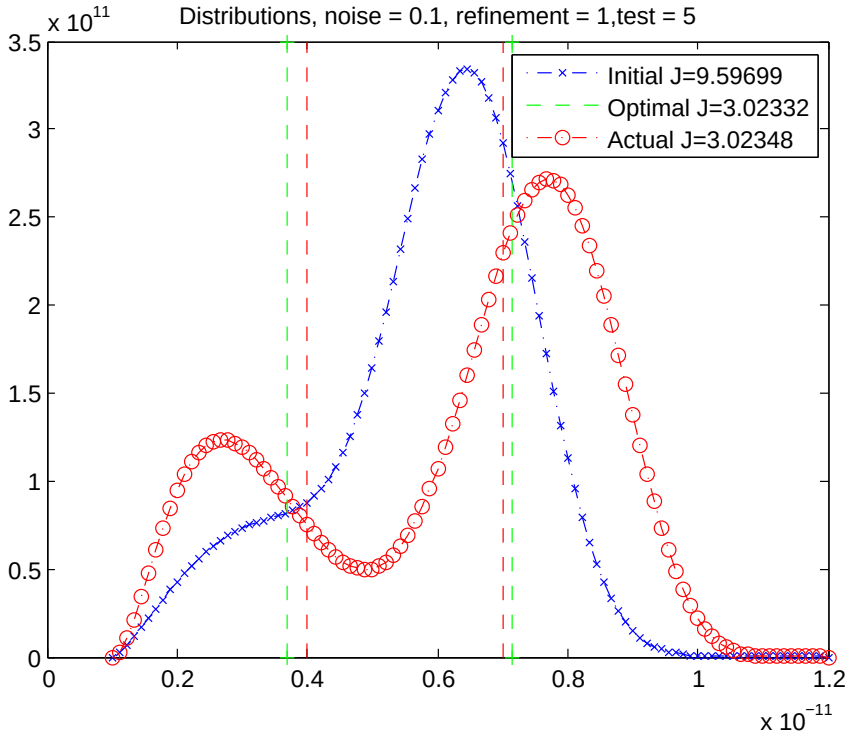


Figure 26: Comparison of Multi-Pole Results to the Distribution using Noise Level 0.1, Refinement of 1, Test 5, Truncated Sine Wave

# 7 Conclusion

Previous work [2] has shown better fits to time-domain data can be achieved by assuming distributions of relaxation times. The work in this paper assumes the distribution of relaxation times follows a beta distribution. We formulate and test the inverse problem to find the distribution of relaxation times of a dispersive dielectric media given time-domain measurements of the electric field at a single receiver.

We are able to determine the mean and standard deviation for a single "usual" Beta distribution with confidence. When the material is a Debye material with a scalar relaxation time, we are able to find a mean close to the actual, while the standard deviation is not exactly zero. In the multi-pole problem, we are able to simulate the electric field with a bi-modal distribution of relaxation times, and are able to gather qualitative information about the distribution, but are not able to completely determine the actual distribution. However, in all cases, the inverse problem finds a good fit to the time-domain data.

This research introduces a way to determine various types of distributions of relaxation times in dispersive dielectrics utilizing Polynomial Chaos methods in the forward simulation. Future work will consist of further analysis of the Debye and multi-pole methods. Also, we would like to further extend this method so that we can test it on real data. By testing with real data, we are able to verify the usefulness of this approach.

# References


[1] H. T. Banks, M. W. Buksas, and T. Lin, *Electromagnetic Material Interrogation Using Conductive Interfaces and Acoustic Wavefronts*, Society for Industrial Mathematics, 2000.

[2] H. T. Banks and N. L. Gibson, *Electromagnetic inverse problems involving distributions of dielectric mechanisms and parameters*, Quarterly of Applied Mathematics **64** (2006), no. 4, 749.

[3] H.T. Banks and N.L. Gibson, *Well-posedness in Maxwell systems with distributions of polarization relaxation parameters*, Applied Math Letters **18** (2005), no. 4, 423–430.

[4] K. Barrese and N. Chugh, *Approximating dispersive mechanisms using the debye model with distributed dielectric parameters*, (2008).

[5] E. Bela and E. Hortsch, *Generalized polynomial chaos and dispersive dielectric media*, (2010).

[6] C. J. F. Böttcher and P. Bordewijk, *Theory of electric polarization*, vol. II, Elsevier, New York, 1978.

[7] K.S. Cole and R.H. Cole, *Dispersion and absorption in dielectrics I. Alternating current characteristics*, The Journal of Chemical Physics **9** (1941), 341.

[8] P. Debye, *Polar molecules*, Dover, 1929.

[9] S. Gabriel, R.W. Lau, and C. Gabriel, *The dielectric properties of biological tissues: III.*, Phys. Med. Biol **41** (1996), no. 11, 2271–2293.

[10] E.R. Von Schweidler, *Studien über anomalien im verhalten der dielektrika*, Ann. Physik **24** (1907), 711–770.

[11] K.W. Wagner, *Zur theorie der unvolkommenen dielektrika*, Ann. Physik **40** (1913), 817–855.

[12] D. Xiu and G. E. Karniadakis, *The Wiener-Askey polynomial chaos for stochastic differential equations*, SIAM Journal on Scientific Computing **24** (2003), no. 2, 619–644.

[13] K. Yee, *Numerical solution of initial boundary value problems involving maxwell's equations in isotropic media*, Antennas and Propagation, IEEE Transactions on **14** (1966), no. 3, 302 –307.

# A Usual Distribution Plots

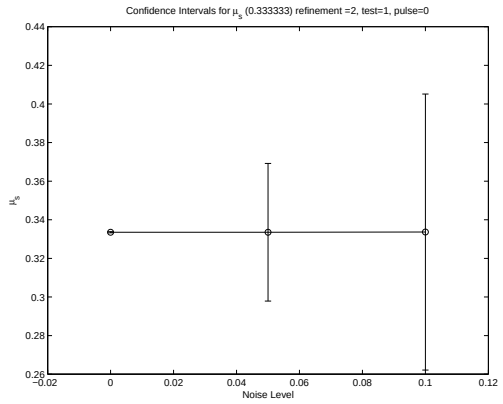


Figure 27: Estimate of Mean using Refinement of 2, Test 1, Truncated Sine Wave

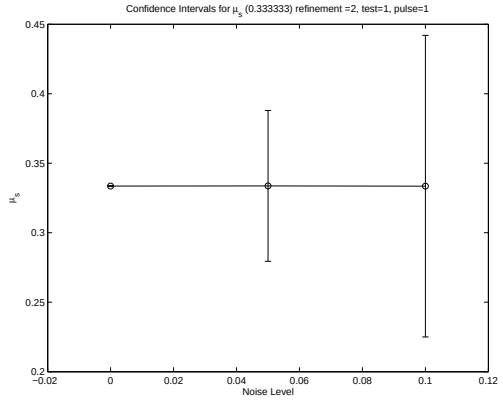


Figure 28: Estimate of Mean using Refinement of 2, Test 1, UWB Pulse

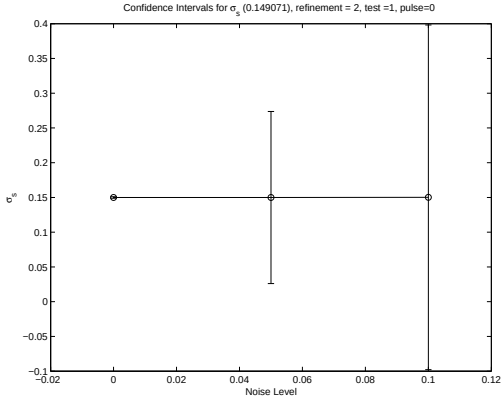


Figure 29: Estimate of Standard Deviation using Refinement of 2, Test 1, Truncated Sine Wave

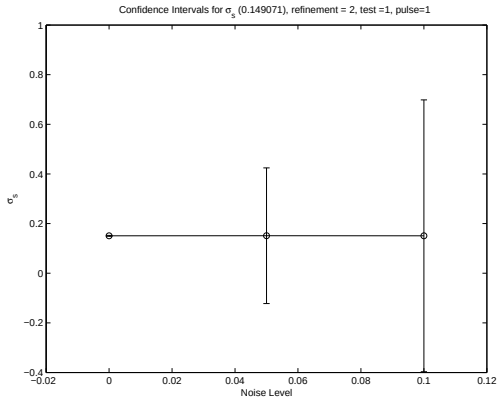


Figure 30: Estimate of Standard Deviation using Refinement of 2, Test 1, UWB Pulse

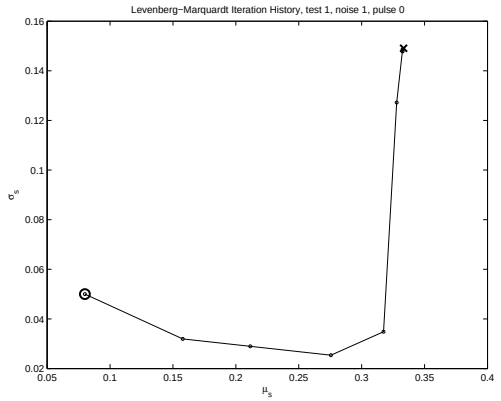


Figure 31: Iteration History using Noise Level 0.1, Refinement of 2, Test 1, Truncated Sine Wave

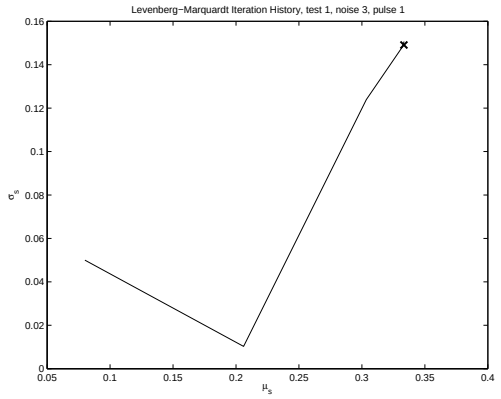


Figure 32: Iteration History using Noise Level 0.1, Refinement of 2, Test 1, UWB Pulse

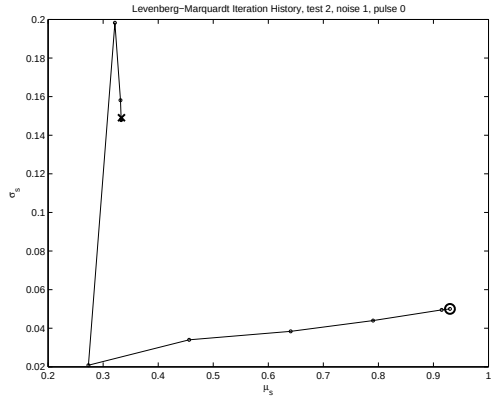


Figure 33: Iteration History using Noise Level 0.1, Refinement of 2, Test 2, Truncated Sine Wave

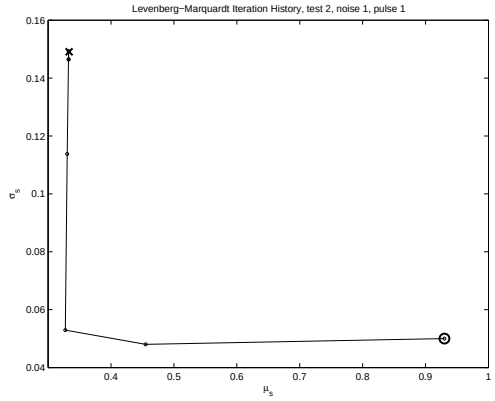


Figure 34: Iteration History using Noise Level 0.1, Refinement of 2, Test 2, UWB Pulse

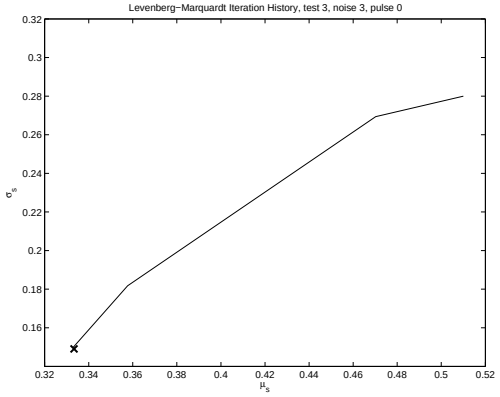


Figure 35: Iteration History using Noise Level 0.1, Refinement of 2, Test 3, Truncated Sine Wave

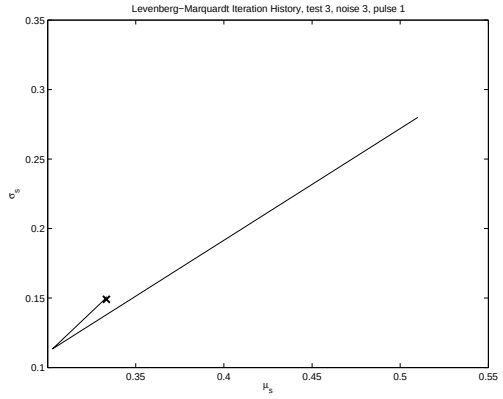


Figure 36: Iteration History using Noise Level 0.1, Refinement of 2, Test 3, UWB Pulse

# B Debye Plots

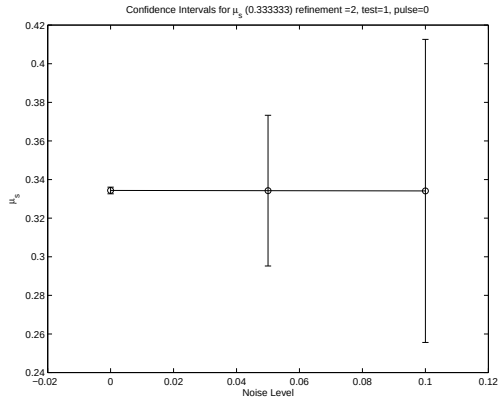


Figure 37: Confidence Intervals for Debye Mean with Refinement of 2, Test 1, Truncated Sine Wave

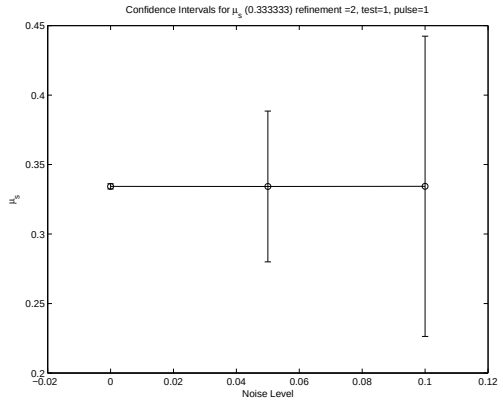


Figure 38: Confidence Intervals for Debye Mean with Refinement of 2, Test 1, UWB Pulse

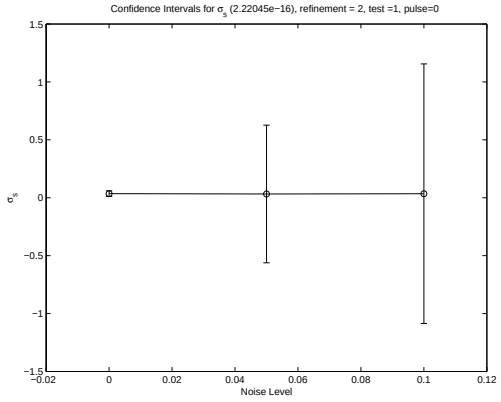


Figure 39: Confidence Intervals for Debye Standard Deviation with Refinement of 2, Test 1, Truncated Sine Wave

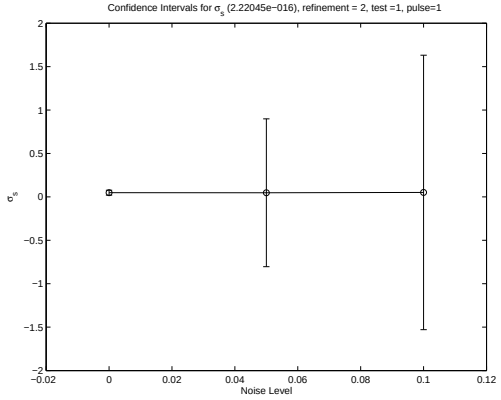


Figure 40: Confidence Intervals for Debye Standard Deviation with Refinement of 2, Test 1, UWB Pulse

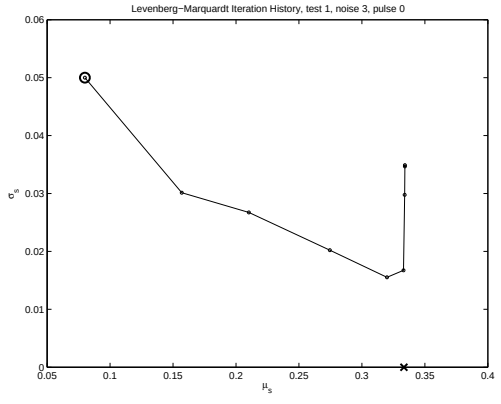


Figure 41: Iteration History for Debye with Noise Level 0.1, Refinement of 2, Test 1, Truncated Sine Wave

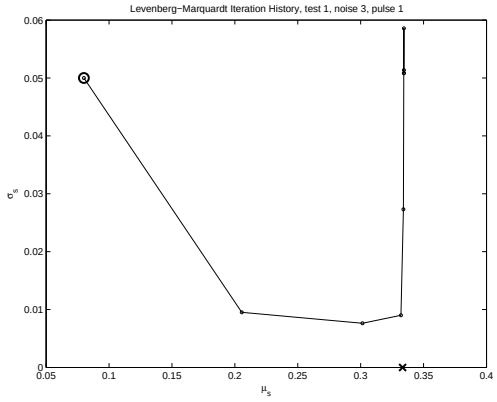


Figure 42: Iteration History for Debye with Noise Level 0.1, Refinement of 2, Test 1, UWB Pulse

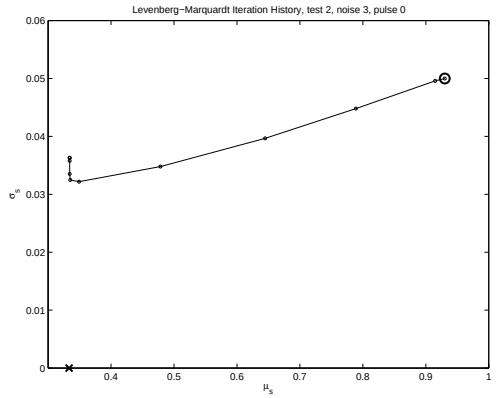


Figure 43: Iteration History for Debye with, Noise Level 0.1, Refinement of 2, Test 2, Truncated Sine Wave

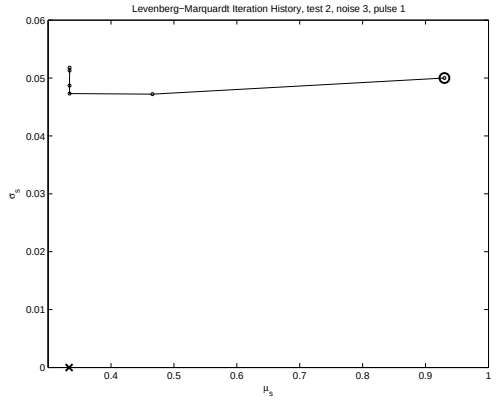


Figure 44: Iteration History for Debye with Noise Level 0.1, Refinement of 2, Test 2, UWB Pulse

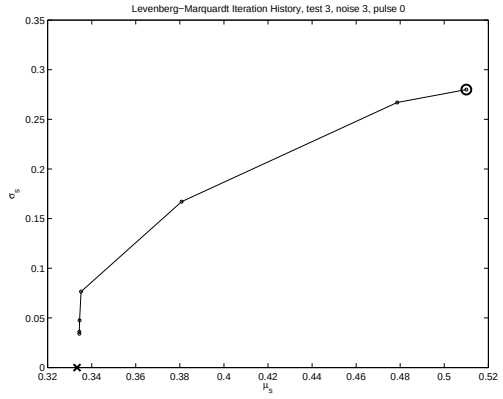


Figure 45: Iteration History for Debye with Noise Level 0.1, Refinement of 2, Test 3, Truncated Sine Wave

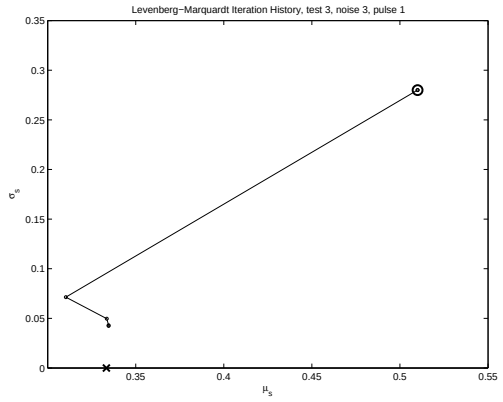


Figure 46: Iteration History for Debye with Noise Level 0.1, Refinement of 2, Test 3, UWB Pulse